



Dual electrochemical genosensor for early diagnosis of prostate cancer through lncRNAs detection

Raquel Sánchez-Salcedo^{a,b}, Rebeca Miranda-Castro^{a,b}, Noemí de-los-Santos-Álvarez^{a,b}, María Jesús Lobo-Castañón^{a,b,*}

^a Departamento de Química Física y Analítica. Universidad de Oviedo, Av. Julián Clavería 8, 33006, Oviedo, Spain

^b Instituto de Investigación Sanitaria del Principado de Asturias, Avenida de Roma, 33011, Oviedo, Spain

ARTICLE INFO

Keywords:

Electrochemical biosensor
Long noncoding RNA
Multiplex detection
PCA3
Prostate cancer

ABSTRACT

The prostate specific antigen (PSA) test is the gold standard for the screening of prostate cancer (PCa), despite its limited clinical specificity. Long noncoding RNAs are released from the tumor tissue to the urine and show great potential for improving specificity in PCa diagnosis. This work reports on a sandwich-type hybridization assay to detect both the urinary biomarker prostate cancer antigen 3 (PCA3) and an endogenous control, the PSA mRNA. Multiple fluorescein-tagged hybridization assistant probes are used to promote the selective capture of this long noncoding RNA, and sensitivity by incorporating multiple redox enzymes per target molecule, after addition of antiluorescein Fab fragment-peroxidase conjugate. This strategy alleviates the problems associated with the low natural abundance of this marker, its large size, and complex secondary structure. The individual genosensors exhibit good sensitivity ($2.48 \pm 0.01 \mu\text{A nM}^{-1}$ and $6.4 \pm 0.3 \mu\text{A nM}^{-1}$ for PCA3 and PSA, respectively), with wide linear ranges (from 25 pM to 10 nM for PCA3 and 1 nM for PSA), and detection limits in the low picomolar range (4.4 pM and 1.5 pM for PCA3 and PSA, respectively). This analytical performance is retained in the dual configuration without significant cross-talk, despite using the same enzyme label. The usefulness of this dual platform was demonstrated by analyzing RNA extracts from the prostate cancer cell line LNCaP and from urine samples of prostate cancer patients.

1. Introduction

As a result of demographic ageing and globalization of unhealthy lifestyles, cancer incidence is steadily increasing, and it does not stop even for a pandemic (Sung et al., 2021). In the particular case of prostate cancer (PCa), the asymptomatic tumor growth makes this cancer a silent enemy. According to the International Agency for Research on Cancer, PCa represents the second most commonly diagnosed cancer and the fifth leading cause of cancer death among men in 2020 (Sung et al., 2021). Early diagnosis is decisive for the survival of patients. It entails the implementation of screening programs based on reliable tests, which provide valuable information with minimum pain and risk. Ideally, the tests should be non-invasive and with a reasonable cost. Liquid biopsy, consisting of the analysis in biological fluids of circulating biomarkers as surrogate material of solid tumors, has the potential to meet these requirements. It may provide valuable information not only for diagnosis but also for the prognosis and follow-up of the disease.

Currently, a serological test measuring prostate specific antigen (PSA), in combination with prostate assessment by digital rectal examination (DRE), is used as an indicator of PCa risk. In case of a high risk, these tests are followed up with a tissue biopsy. However, despite its acceptable clinical sensitivity, the PSA test has a limited clinical specificity. This leads to unnecessary biopsies and overtreatment of indolent tumors. As a result, in 2008 PSA-based screening for PCa was discouraged in the USA. However, in 2017 it was partially amended (Catalona, 2018).

Prostate Cancer Antigen 3 or PCA3 is an alternative biomarker for prostate cancer diagnosis to distinguish between aggressive and non-aggressive disease. First identified in 1999 as Differential Display Clone 3 or DD3 (Bussemakers et al., 1999), PCA3 is part of the large percentage of human transcriptome not involved in protein synthesis. Due to its size longer than 200 nucleotides, PCA3 falls into the category of long noncoding RNAs (lncRNAs) (Bhan et al., 2017; Miranda-Castro et al., 2019).

* Corresponding author. Departamento de Química Física y Analítica. Universidad de Oviedo, Av. Julián Clavería 8, 33006, Oviedo, Spain.

E-mail address: mjlc@uniovi.es (M.J. Lobo-Castañón).

<https://doi.org/10.1016/j.bios.2021.113520>

Received 22 May 2021; Received in revised form 5 July 2021; Accepted 15 July 2021

Available online 21 July 2021

0956-5663/© 2021 The Author(s).

Published by Elsevier B.V. This is an open access article under the CC BY-NC-ND license

(<http://creativecommons.org/licenses/by-nc-nd/4.0/>).

Unlike PSA protein serum levels, PCA3 expression has been reported to be PCA specific. It is unaffected by other benign prostate conditions, thus becoming one of the most PCA specific biomarkers identified so far (Lemos et al., 2019). It has been detected in prostate tumor tissues, peripheral blood and urine after DRE. Urine-based tests are preferable because of the physical proximity to the prostate, in addition to the low urinary protein levels and the possibility of truly noninvasive repeated sampling (Peng et al., 2017). Therefore, PCA3 has been approved by the US Food and Drug Administration (FDA) as a urinary marker for prostate cancer diagnosis (Sartori and Chan, 2014), being the only lncRNA to achieve it so far.

The diagnostic potential of PCA3 has been typically evaluated by reverse transcription quantitative PCR (RT-qPCR) with fluorescence detection (de Kok et al., 2002; Hessels et al., 2003). Trying to overcome its intrinsic drawbacks, reverse transcription loop-mediated isothermal amplification (RT-LAMP) coupled with colorimetric detection has been proposed (Wang et al., 2020). Likewise, RT-PCR involving thiolated primers has been combined with unmodified gold nanoparticles for colorimetric detection of PCA3. A change in color from red to blue resulting from salt-induced aggregation indicates the absence of PCR amplification and consequently of PCA3 (Htoo et al., 2019). However, these colorimetric methods do not consider the variable number of prostate cells released into the sample, as in traditional RT-qPCR methods.

A quantitative PCA3 test commercialized by ProgenSA has been approved by US FDA to guide the decision regarding repeated biopsies (Groskopf et al., 2006). It is based on the isothermal amplification of PCA3 by transcription mediated amplification (TMA) and subsequent hybridization-based chemiluminescence detection. Urine PCA3 levels are normalized to the amount of PSA mRNA to obtain a PCA3 score. It requires specific and sophisticated equipment, and personnel proficient in its use. This has limited its application to private clinics.

Therefore, there is a clear need for simpler, reliable and cost-effective methods for the detection of PCA3. Nucleic acid-based electrochemical biosensors are a very promising alternative for the clinical implementation of liquid biopsy (Miranda-Castro et al., 2020; Das and Kelley, 2020; Bellassai and Spoto, 2016), with potential to meet those demands. They combine the selectivity of the biomolecular recognition event (i.e. hybridization between complementary strands) with the high sensitivity, rapid response, simple use and portability of electrochemical transducers. Moreover, electrochemical detection offers the possibility of multiplexed detection, which is of great importance for clinical diagnosis (Labib et al., 2016). The simultaneous detection of multiple circulating biomarkers has proven to be more efficient for cancer screening. But also, to control the misexpression of genetic biomarkers, it is imperative to normalize the values with respect to a transcript with stable expression (a housekeeping gene transcript serving as an internal standard). This is the only way to exclude any non-cancer related variations. It entails the development of dual approaches. However, to date, none of the electrochemical genosensors for the detection of PCA3 (Rodrigues et al., 2021; Soares et al., 2019) posed a dual approach. In this work, to facilitate PCA screening, we propose a dual electrochemical hybridization-based biosensor with enzymatic signal amplification for the determination of PCA3 and PSA mRNA as an endogenous control.

2. Materials and methods

2.1. Preparation of the modified SPECs

Two different designs of screen-printed electrochemical cells (SPECs) were employed for genosensors fabrication, both including a silver pseudo-reference electrode and a gold counter electrode (Metrohm DropSens, Spain). Single genosensors were developed onto SPECs with a circular gold working electrode of \varnothing 4 mm (SPAuECs, DRP-220BT). Dual genosensors were built onto SPECs involving two elliptic gold working electrodes (SPdAuECs), with major and minor axes of 3.5 and 1.75 mm,

resulting in a geometric area of 4.8 mm². The SPECs were cleaned with ethanol and Milli-Q water, and dried under a stream of nitrogen. Afterwards, an electrochemical conditioning of the gold working electrodes was conducted by cyclic voltammetry in 0.5 M H₂SO₄ (40 μ L onto the SPEC). The potential was cycled between 0 and +1.3 V at 100 mV/s until a stable voltammogram was recorded (~10 cycles). Then, the SPECs were washed thoroughly with Milli-Q water and dried with nitrogen immediately before modification with the sensing layer.

The thiolated capture probe (CP-PCA3 for PCA3 or CP-PSA for PSA), along with the auxiliary capture probe (AuxCP-PCA3) in the case of PCA3, were dissolved in 2 \times SSPE buffer solution pH 7 to a final concentration of 1 μ M each to form the corresponding partial duplex (hereinafter referred to as the thiolated capture structure). The mixture was heated at 95 $^{\circ}$ C for 5 min and gradually cooled down to room temperature. The conditioned working electrodes were covered with this solution and incubated overnight at 4 $^{\circ}$ C in a humidified atmosphere to allow the thiolated capture structure to chemisorb onto the gold surface. Subsequently, a 50 min incubation step with *p*-aminothiophenol (1 mM in 2 \times SSPE buffer solution pH 7) was performed at RT to displace nonspecifically attached oligonucleotides and block the bare gold surface. Unbound aromatic thiol was then removed by washing with 2 \times SSPE buffer solution pH 7.

2.2. Sandwich assay

The specific recognition of the target (PCA3 or PSA) was carried out through two successive hybridization steps. First, 0.2 μ M of each detection probe labeled with 6-carboxyfluorescein (DP₁₃, DP₁₅, DP₁₆, DP₂₀, and DP₂₁ for PCA3, DP₁₉ and DP₂₂ for PSA) and varying concentrations of the target (T_{PCA3} or T_{PSA}) in hybridization buffer (2 \times SSPE, pH 7) were heated at 95 $^{\circ}$ C (70 $^{\circ}$ C for RNA samples) for 5 min, and immediately cooled in ice. After bringing the mixture to RT, the same volume of 5 % BSA in hybridization buffer was added, giving rise to a final concentration of 2.5 % BSA and 0.1 μ M of each detection probe. This solution (10 μ L) was deposited onto the sensing surface and incubated at RT for 2 h in the darkness. Then, the surface was washed with hybridization buffer, dried with N₂ and, after a 10 min conditioning step with blocking buffer (0.5 % casein 1 \times PBS), the modified electrode was incubated with 10 μ L of anti-fluorescein-Fab fragment peroxidase conjugate (antiF-POD, 0.5 U/mL) in blocking buffer for 30 min and protected from the light at RT. The excess of enzyme conjugate was removed by washing with 2 \times SSPE buffer solution pH 7, and the surface was dried with nitrogen just before electrochemical quantification of the immobilized enzyme activity. For that purpose, 40 μ L of the TMB substrate solution including H₂O₂ was added onto the complete electrochemical cell. After 60 s of enzymatic reaction, the oxidized form of TMB generated was electrochemically reduced by application of 0 V for 60 s, and the steady-state current signal was employed as the analytical signal. The chronoamperometric measurements using the dual sensors were carried out simultaneously.

2.3. RNA extraction from cells

Total RNA was collected from LNCaP or PC-3 cell pellets previously thawed at RT by using the EZNA Total RNA Kit I (Omega Bio-tek, USA) according to the manufacturer's protocol. Briefly, the extraction is based on the lysis of the cells by using a buffer containing guanidinium thiocyanate and subsequent homogenization of the lysate before transferring to silica spin columns. After washing steps with the recommended buffers, the RNA is eluted with RNase free water preheated at 70 $^{\circ}$ C by centrifugation at maximum speed (\geq 12,000 g) for 2 min.

Total RNA concentration was spectrophotometrically determined (SimpliNanoTM spectrophotometer, Thermo Fisher Scientific, Madrid, Spain) at 260 nm, considering that 1 absorbance unit corresponds to 40 ng/ μ L RNA. RNA purity and integrity was evaluated by using an

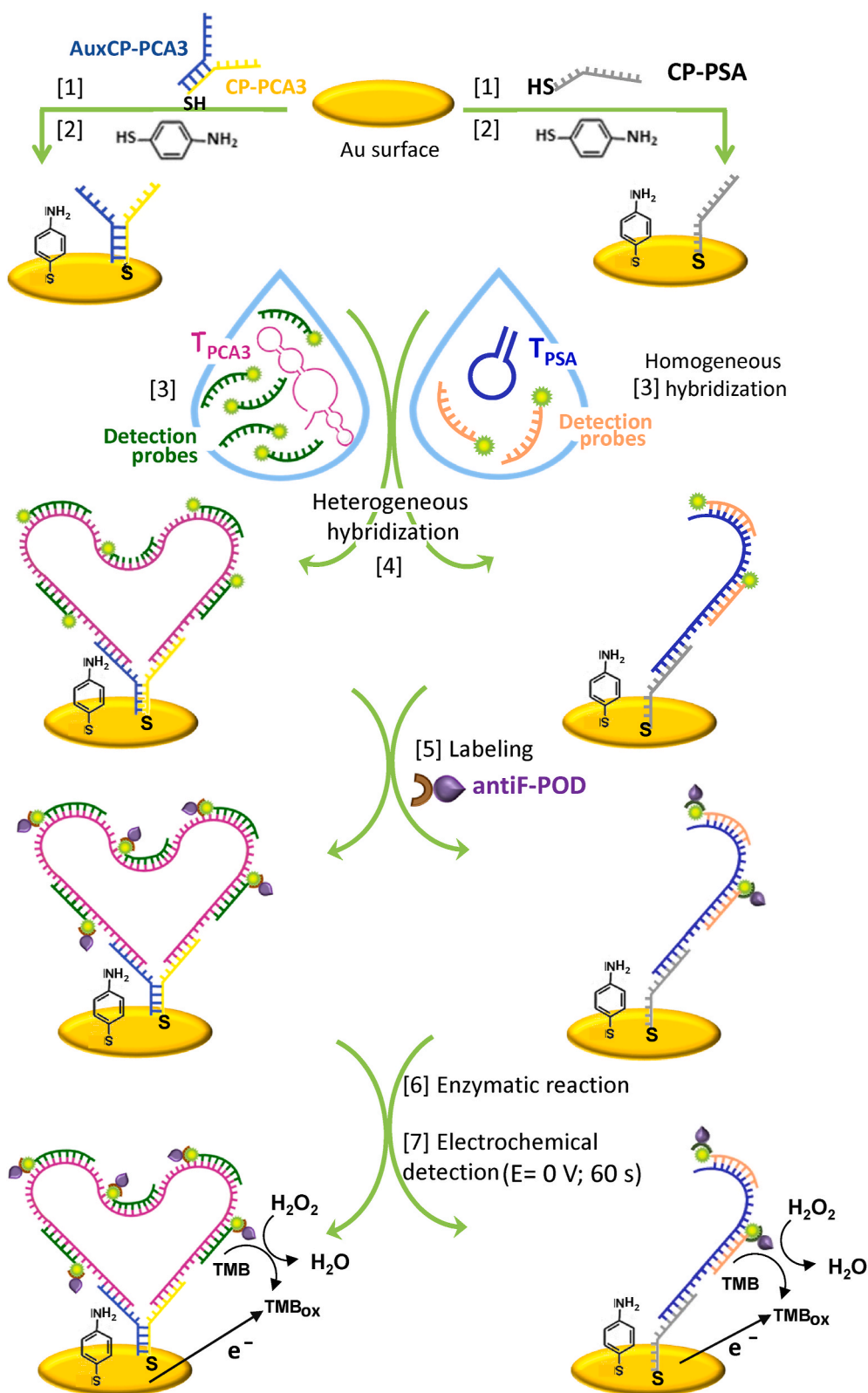


Fig. 1. Steps involved in the construction and operation with the electrochemical genosensor for PCA3 (left) or PSA (right): (1) chemisorption of the thiolated capture structure; (2) blocking with *p*-aminothiophenol; (3) homogeneous hybridization between the target and the fluorescein-tagged detection probes; (4) heterogeneous hybridization; (5) enzymatic labeling with antiF-POD conjugate; (6) enzymatic reaction; (7) chronoamperometric detection.

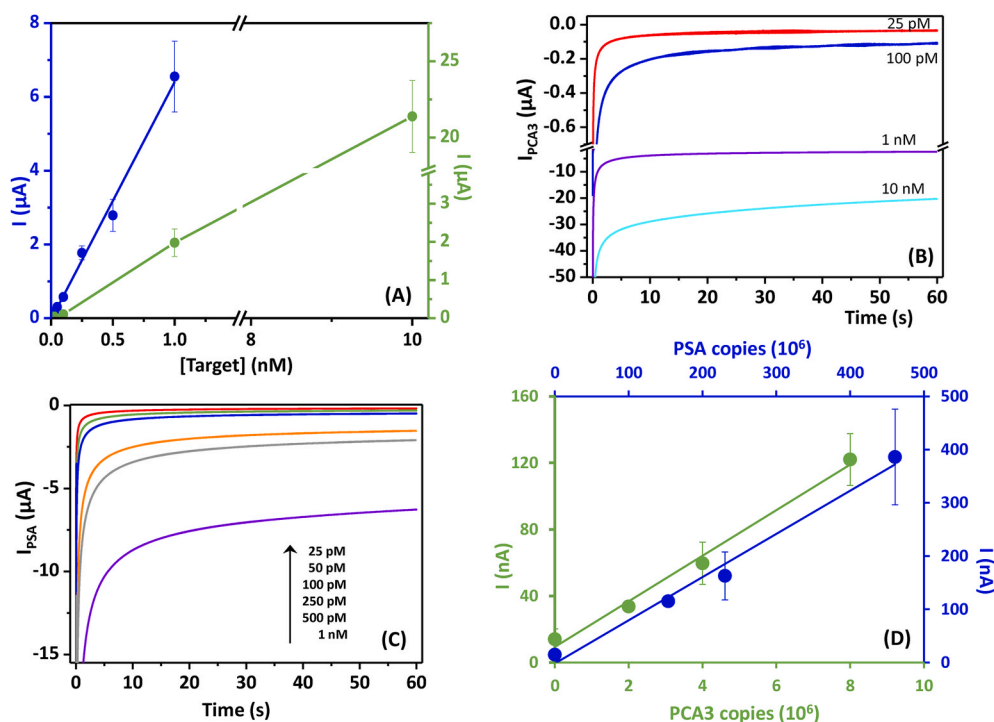


Fig. 2. (A) Calibration plots for the determination of the synthetic targets T_{PCA3} (green) and T_{PSA} (blue). (B) Chronoamperometric response of PCA3 genosensor incubated with different concentrations of T_{PCA3} . (C) Chronoamperometric response of PSA genosensor incubated with different concentrations of T_{PSA} . (D) Variation of the current intensity recorded for serial dilutions of LNCaP extracts with the estimated number of copies of PCA3 lncRNA (green) and PSA mRNA (blue). The error bars represent the standard deviation of at least three independently fabricated sensors. (For interpretation of the references to color in this figure legend, the reader is referred to the Web version of this article.)

automated microfluidic gel electrophoresis platform (Bioanalyzer 2100 Agilent, Madrid, Spain).

2.4. Magnetic isolation of PCA3 and PSA RNAs

The purification of the samples was performed by using streptavidin-functionalized magnetic microparticles (MPs) previously modified with target-specific biotinylated probes (baits). For that, a 100 μ L aliquot of commercial MPs (10 mg/mL, 1 mg) was transferred to a vial and washed twice with the washing buffer (5 mM Tris-HCl, 1 M NaCl, 0.01 % Tween, pH 7.4). Then, MPs were suspended in 500 μ L of 1 \times binding buffer (5 mM Tris-HCl, 1 M NaCl, pH 7.4) containing the corresponding biotin-labeled bait at 2 μ M and incubated for 30 min at RT with gentle agitation in a Dynabeads™ MX 12-tube Mixing Wheel (Thermo Fisher Scientific, Madrid, Spain). After supernatant removal the modified MPs were washed with the washing buffer, resuspended in 600 μ L of 2 \times binding buffer, and kept at 4 $^{\circ}$ C until usage.

The isolation of PSA and PCA3 RNA (in this order) from cell lysates was carried out as follows: 600 μ L of Bait-PSA modified MPs were added to 600 μ L of cell lysate. The mixture was incubated for 30 min at 46 $^{\circ}$ C and 1000 rpm. Then, MPs were magnetically entrapped and the supernatant was transferred to a clean tube for subsequent capture of PCA3, applying the same protocol with Bait-PCA3 modified MPs. Both batches of MPs were washed twice and the elution of PSA and PCA3 RNA was performed in parallel with 50 μ L nuclease-free water by incubation at 70 $^{\circ}$ C for 2 min. Both eluates were combined and the mixture (100 μ L) was evaporated to 20 μ L. The resulting RNA solution was stored at -80° C for further analysis.

2.5. Urine samples acquisition and treatment

Urine samples from 4 PCa patients identified with positive biopsy were provided by the Department of Urology at Hospital Universitario Central de Asturias (Oviedo, Spain). Written informed consent was given by patients. 5-mL first catch urine was obtained after DRE and centrifuged at 4 $^{\circ}$ C and 700 g for 10 min. After removal of the supernatant, the pellet was washed with phosphate-buffered saline and stored at -80° C. Before analysis with the electrochemical genosensors, each cell pellet

was thawed on ice, treated with 700 μ L lysis buffer (according to the manufacturer's recommendations) and subjected to the specific entrapment of PSA and PCA3 RNAs using magnetic microparticles, as previously described for cell lines.

3. Results and discussion

3.1. Design and optimization of sandwich PCA3 lncRNA genosensors

The analysis of PCA3 using hybridization-based biosensors presents three important challenges. First, the large size of this lncRNA (from 3622 to 3922 nucleotides, depending on the variant) negatively affects its diffusion through the solution towards the sensing platform. Closely related to the previous one is the internal secondary structure of the target that hinders the hybridization with the surface-confined capture probe, resulting in low hybridization efficiency. The third one is the low abundance of the transcript, even when overexpressed in cancer patients.

To address these issues, we propose the incorporation of short DNA fragments serving as hybridization assistant probes. In-solution interaction of these probes with the long target sequence disrupts its secondary structure, thus facilitating its selective capture onto the sensing platform. Moreover, appropriate modification of the probes enables to accommodate multiple redox enzymes per target molecule, with the consequent signal amplification, turning them into detection probes as well.

We have selected a specific sequence of 190 nucleotides as the PCA3 target, which takes part in the exon 4 of the PCA3 gene (see Section S1.3). The target structure predicted by Mfold software (Zuker, 2003) exhibits two regions with extensive secondary structure (Fig. S1). Five detection probes modified with 6-carboxyfluorescein (6-FAM) at the 3' end were designed to hybridize with specific parts of the target. Each detection probe was named as DP_N, where the subscript N indicates the number of nucleotides. In particular, DP₂₀, DP₂₁, and DP₁₃ disrupt the secondary structure of region I, while the structured region II is unfolded with DP₁₅ and DP₁₆ (Fig. S1). Despite not being optimal (Miranda-Castro et al., 2007), the resulting sandwich structure is not a continuous duplex. This is somewhat imposed by the very strong secondary

Table 1
Comparison of hybridization-based assays for PCA3 lncRNA detection.

Reference	Target	Sensing platform/assay format	Transduction	Signal amplification	LOD	Sample/Normalization
Soares et al. (2019)	Synthetic DNA (21mer)	LbL chitosan and MWCNTs onto Au electrodes Direct assay	EIS	–	128 pM	Total RNA from LNCaP (control PC3 and HeLa)/No endogenous
Rodrigues et al. (2021)	Synthetic DNA (21mer)	LbL AuNPs-CS onto C electrodes Direct assay	EIS	–	83 pM	Buffer spiked with synthetic DNA/No endogenous
Vilela et al. (2017)	Synthetic DNA (20 mer)	Graphene oxide- CapProbe- upconversion NPs/Direct	Optical	–	0.5 pM	Plasma and lysates from healthy volunteers/No endogenous
Siooss et al. (2012)	Synthetic DNA (45 mer) or <i>in vitro</i> transcribed PCA3 RNA	Silica coated nanowires-ASOs/Sandwich	Optical (resonance frequency shifts)	ASOs-AuNPs	–	Peripheral blood spiked with target/No endogenous
Fu et al., 2019	Synthetic DNA (40 mer)	Strep-Biotin-DNA Cap Probe onto a membrane + AuNPs with MGITC & Thiol-DNA ReporterProbe/Displacement	SERS-based Lateral Flow Assay	–	3 fM	Spiked serum and 5 times dilution No endogenous
This work	Synthetic DNA (190 mer)	Thiol-DNA probe/Sandwich	Chronoamperometry of TMB	Enzyme amplification	4.4 pM	Selective capture of PCA3 and PSA mRNA from cell lysates

EIS: electrochemical impedance spectroscopy; LbL: layer by layer technology; MWCNTs: multiwall carbon nanotubes.

AuNPs: gold nanoparticles; ASO: antisense oligonucleotide; SERS: Surface-enhanced Raman scattering; MGITC: malachite Green.

structure of the target, since the use of longer detection probes could lead to very stable hybrids between them that would compete with the formation of the desired complex. This feature was, however, used to improve the capture efficiency. More specifically, we designed a y-shape capture structure generated by hybridization between a thiolated capture probe containing a spacer of 6 thymines, CP-PCA3, and an auxiliary capture probe with a spacer of 6 adenines, AuxCP-PCA3 (Table S1). Such a capture structure hybridizes with both ends of the target due to the flexibility that the imperfect duplex possesses.

The complete scheme of the genosensor is depicted in Fig. 1. The sensing layer selective to PCA3 consists of a binary self-assembled monolayer (SAM) built onto gold surfaces by chemisorption of the thiolated y-shape capture structure performed in solution and *p*-aminothiophenol. This strategy provides very low background signals (Miranda-Castro et al., 2018), which is crucial for the detection performance. It hybridizes with the duplex generated in solution between the target and the five detection probes tagged with 6-FAM. The resulting complex is then treated with the enzyme conjugated antiF-POD to fix multiple redox enzymes per each hybrid formed onto the sensing surface. Finally, the immobilized enzymatic activity, which is directly proportional to the target concentration in the tested solution, is measured by chronoamperometry.

The development and optimization of the electrochemical genosensor was performed by using a DNA analog, T_{PCA3}, to avoid misleading conclusions arising from RNA instability.

We initially attempted to generate T_{PCA3} by PCR from commercial cDNA, by using a suitable set of primers. Nevertheless, unlike for shorter duplexes (Barreda-García et al., 2018), the resulting 190 bp amplicon was too stable to hybridize with the capture and detection probes. This fact points to the need for working with the target in single-stranded form, what resembles more closely the ultimate goal of this work, i.e. the determination of the PCA3 lncRNA. Therefore, the synthetic target T_{PCA3} was used as a calibrator.

The sensitivity of the electrochemical biosensing platform for PCA3 quantification was investigated by recording the reduction current of the enzymatically oxidized TMB at 0 V. As illustrated in Fig. 2A–C, the current intensity linearly increases with increasing T_{PCA3} concentration in the range from 25 pM to 10 nM ($I/\mu\text{A} = (2.48 \pm 0.01) [\text{T}_{\text{PCA3}}]/\text{nM} - (0.03 \pm 0.07)$; $r = 0.99997$; $n = 4$). The assay reproducibility was 17 % across the dynamic range stated above, and the detection limit, calculated as three times the standard deviation of the blank signal divided by the slope of the regression equation, was 4.4 pM. This value is competitive or even superior to previously reported PCA3 biosensors, even if they were developed by using shorter synthetic targets (Table 1).

The usefulness of the auxiliary capture probe AuxCP-PCA3 in PCA3 determination was investigated at 1 nM of T_{PCA3}. The cathodic current recorded when this probe takes part in the sensing layer was more than twofold the signal obtained in its absence, thus evidencing its important role in method sensitivity. Afterwards, we evaluated the significance of the five detection probes by comparing their signal contribution. The experimental results pointed out that the analytical signal does not increase linearly with the number of detection probes, since around 46 % of the total current intensity is provided by the probe DP₁₆ (Fig. S2). It might be attributed to the different stability of the secondary structure of regions I and II in the target structure.

3.2. Design and optimization of sandwich PSA mRNA genosensor

Considering that PCA3 signal will be affected by the number of prostate cells released to the male urine during the DRE, normalization to an internal RNA control is needed for reliable PCA3 quantification and exclusion of any nonspecific variation. With this purpose, PSA mRNA was selected as endogenous control, as its expression levels are not altered by prostate cancer (Magklara et al., 2000. Meng et al., 2002). A sandwich hybridization assay was designed for this transcript (Fig. 1). A specific fragment of 66 nucleotides called T_{PSA} was chosen to hybridize in solution with two detection probes, DP₁₉ and DP₂₂, and the resulting DNA trimeric structure is subsequently captured onto a binary SAM consisting of a thiolated capture probe specific of T_{PSA}, CP-PSA, interspersed with *p*-aminothiophenol.

The analytical performance of T_{PSA} genosensor was then assessed, applying a procedure equivalent to that for T_{PCA3} genosensor. The linear regression equation was found to be $I/\mu\text{A} = (6.4 \pm 0.2) [\text{T}_{\text{PSA}}]/\text{nM} - (0.0 \pm 0.1)$ within the range 0.025–1 nM, with a correlation coefficient of 0.996. Likewise, PSA mRNA genosensor exhibits a detection limit of 1.5 pM with an average RSD of 16 %.

3.3. Detection of PCA3 and PSA mRNA in prostate cancer cell lines

When comparing the slopes of the calibration curves for T_{PCA3} and T_{PSA}, i.e. the sensitivity, it is striking that the value for the T_{PCA3} genosensor using five detection probes is around 2.6 times lower than the value for the T_{PSA} genosensor involving two detection probes. This unexpected finding could be related to the greater complexity of T_{PCA3} with respect to T_{PSA} (longer length and stronger secondary structure), which is a reflection of their natural RNA counterparts. To clarify the pertinence of employing five detection probes for PCA3 determination, we challenged the electrochemical genosensor with the total RNA extracted

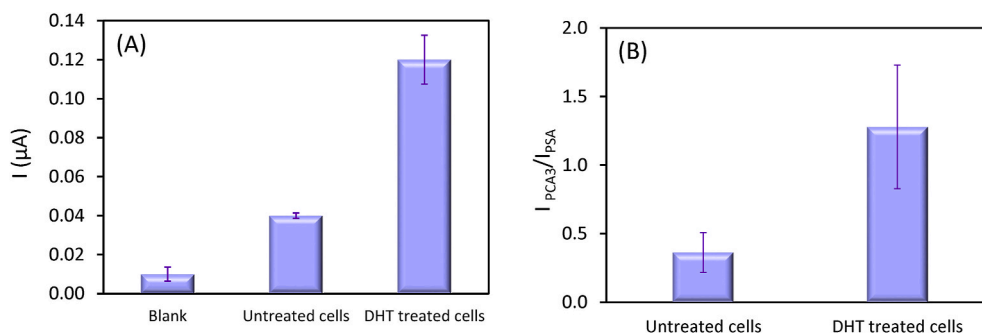


Fig. 3. Androgen stimulation of PCA3 in LNCaP cells by treatment with 70 nM DHT for 24 h. (A) Signal recorded with PCA3 genosensor for treated and untreated cells. (B) Ratio of PCA3 to PSA signals for treated and untreated cells.

from cultures of the human prostate cancer cell line LNCaP (see Sections S1.4 and 2.3). The analytical signal recorded when using five detection probes was almost five times higher than that obtained with two detection probes, while the background signal remained virtually the same, thereby demonstrating the clear benefits of the proposed design.

Subsequently, the response exhibited by the sandwich-type genosensors towards PCA3 and PSA RNAs from LNCaP lysates was investigated in greater depth. Fig. 2D shows the analytical signal recorded from serial dilutions (2-fold) of the same cell lysate. A linear variation of the current intensity as a function of the number of PCA3 or PSA copies was found. Notice that the number of RNA copies was estimated considering that one LNCaP cell contains 10 PCA3 copies and 1500 PSA mRNA copies (Groskopf et al., 2006). However, when analyzing different cell lysates, a clearly defined trend of the response was lacking. It might be attributed to selectivity problems (presence of a large quantity of RNA among which PCA3 and PSA RNAs are minority) or to the uncertainty in cell counting which makes the cell pellets not comparable in quantitative terms.

To clarify this question, we entrapped the targets with streptavidin-coated magnetic beads modified with a 40 polyT oligonucleotide through A-T pairing, taking advantage of the fact that both are polyadenylated. After elution at 70 °C, the genosensor signal decreased sharply. This was attributed to saturation of the particles with other abundant RNAs harboring a polyA tail which are not recognized by the sensing layers. These results highlight the good selectivity of the genosensors.

Subsequently, specific entrapment was conducted with streptavidin-functionalized MPs previously modified with biotinylated probes complementary to a target fragment unrecognized by the genosensor and referred to as bait. They include a spacer of 10 adenines (Bait-PCA3 and Bait-PSA for PCA3 and PSA, respectively). Elution and detection steps were not modified. Cell pellets containing between 7×10^5 and 2.5×10^6 LNCaP cells (rough estimation with a hemocytometer) gave rise to net signals corresponding to the mid to low concentration region in both calibrations. The PCA3 to PSA signals ratio was 0.46 ± 0.08 .

In order to check that the recorded signals are indeed related to the amount of PCA3 present, we implemented the androgen stimulation of PCA3. Significant upregulation of PCA3 expression in LNCaP cells has been previously reported as a result of their treatment with dihydrotestosterone (DHT) (Ferreira et al., 2012). Accordingly, LNCaP cells were cultured in the regular medium until a suitable cell density was achieved (70–75% confluence). Then, the medium was replaced by fresh one containing 70 nM DHT, and the cells were allowed to grow for a further 24 h. The resulting cell pellet was isolated and subjected to the usual analysis procedure, and the electrochemical response was compared with that obtained for a similar number of untreated cells processed in parallel. From Fig. 3A, a significant increase in the PCA3 electrochemical signal arisen from androgen stimulation is apparent, while the effect on PSA mRNA signal was negligible. Particularly, the ratio of PCA3 to PSA signals enhanced by a factor of 3.5 (Fig. 3B).

Table 2

Analysis of clinical urine samples: PCA3 to PSA signals ratio and threshold cycle (C_T) for RT-qPCR of PSA mRNA.

Sample	Diagnosis	$I_{\text{PCA3}}/I_{\text{PSA}}$	C_T (PSA)
1	PCa	1.5 ± 0.2	35.4
2	PCa	1.2 ± 0.3	32.8
3	PCa	1.2 ± 0.9	37.0
4	PCa	<LOD	>40

Changes in the PCA3 expression after treatment with DHT were also evaluated by reverse transcription-quantitative polymerase chain reaction (RT-qPCR) according to the $2^{-\Delta\Delta C_T}$ method (Livak and Schmittgen, 2001), using PSA mRNA as internal control and untreated LNCaP cells as reference sample. Assuming that amplification efficiencies of target and control are approximately equal, a fold change of 55 was found. Therefore, both the electrochemical genosensor and RT-qPCR evidence an overexpression of PCA3 lncRNA in LNCaP cells induced by DHT.

Selectivity studies were subsequently performed with the RNA extracted from PC-3, an androgen-insensitive prostate cancer cell line that does not express neither PCA3 nor KLK3 genes (Tai et al., 2011). The chronoamperometric responses recorded with PCA3 and PSA genosensors were not significantly different from the corresponding background signals (Fig. S3), thus confirming the good selectivity of the electrochemical genosensors developed herein.

Finally, the electrochemical method was applied to the detection of PCA3 in urine samples. The specimens were subjected to cell lysis, entrapment of PSA and PCA3 RNAs with MPs functionalized with specific probes (baits), eluted with hot RNase-free water, and analyzed using the described electrochemical method. Likewise, the quality of the RNA extraction was checked by PSA mRNA amplification. First, woman urine was evaluated. The signals recorded with both biosensors matched, within the experimental error, those obtained for the blank. Therefore, sample matrix does not significantly affect the response of the biosensors. Then, urine samples from four patients with biopsy confirming PCa were assessed. In three of the four cases the ratio of PCA3 to PSA signals was superior to one (Table 2), in line with the results obtained for DHT-stimulated LNCaP cells. A value lower than the detection limit was recorded for the fourth one, which was concordant with the absence of PSA mRNA amplification by RT-PCR, probably pointing out insufficient cell sediment in the collected sample. This also emphasizes the importance of using an internal standard for reliable determination of PCA3 in urine.

3.4. Dual platform for simultaneous detection of PCA3 and PSA RNAs

We envisaged the possibility of implementing both individual genosensors in the same biosensing platform. For such a purpose, we selected dual screen-printed electrochemical cells (SPdAuECs) consisting of two elliptic gold working electrodes sharing the Ag-

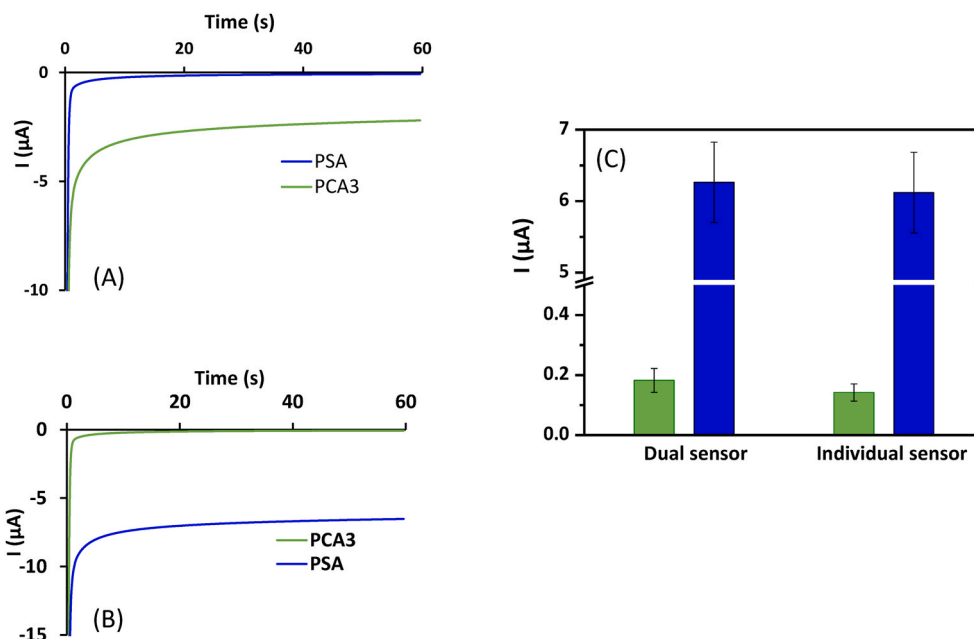


Fig. 4. Cross-talk evaluation in dual sensing platforms. Electrochemical response of PCA3 genosensor (green) and PSA genosensor (blue) incubated with a mixture of: (A) 1 nM T_{PCA3} and 0 nM T_{PSA} , (B) 0 nM T_{PCA3} and 1 nM T_{PSA} . (C) Comparison of the analytical signal recorded for 100 pM T_{PCA3} and 1 nM T_{PSA} when using single or dual sensors. (For interpretation of the references to color in this figure legend, the reader is referred to the Web version of this article.)

pseudoreference and the Au-counter electrode in the same strip. This configuration poses important challenges associated with the biomolecular recognition and electrochemical transduction steps. First, we performed *in silico* analyses of the capture and detection probes that take part in both genosensors to identify possible undesired interactions between them that could negatively affect the genosensors performance. Thermodynamic predictions carried out with MFold software (Zuker, 2003) ruled out this scenario.

Regarding the transduction step, Wang and coworkers have recently reported a dual enzymatic electrochemical immunosensor for simultaneous detection of two hormones, by using two different enzymes without interference of the reaction products at neighboring electrode (Vargas et al., 2020). This approach, however, entails adopting compromise operational parameters, instead of applying the optimum conditions in each case. Conversely, in the present work both genosensors involve the same redox enzyme and procedure to quantify the immobilized enzymatic activity, thus favoring their integration. Nevertheless, the measurement of the same enzymatic product could give rise to cross-talk by diffusion of oxidized TMB between the two working electrodes. This possibility was investigated by exposing the dual sensing platforms to a high concentration of one biomarker in the absence of the other one. As illustrated in Fig. 4A and B, in neither case false positives were obtained. Moreover, the simultaneous electrochemical readout of the two targets at different concentration levels matches, within the experimental error, the values recorded with the corresponding single genosensors (Fig. 4C).

Finally, the response of the dual biosensing platform was evaluated against LNCaP cell lysates with or without a previous treatment with DHT, obtaining a PCA3 to PSA signals ratio of 1.39 and 0.42, respectively. These values are in line with those recorded with the single biosensing platforms, thus demonstrating the feasibility of the dual electrochemical sensing platform.

4. Conclusions

A dual electrochemical biosensor for simultaneous detection of PCA3 lncRNA, a urinary biomarker of prostate cancer, and PSA mRNA, serving as internal standard, has been developed. It has been accomplished by

integration of two sandwich-type hybridization assays involving multiple detection probes to incorporate several redox enzymes per analyte captured onto the sensing layer. This signal amplification strategy allows the reliable quantification of synthetic PCA3 at picomolar levels (LOD = 4.4 pM and %RSD = 17 %). By combining the dual biosensing platform with a previous capture and preconcentration step with magnetic particles modified with sequence-specific probes is possible to determine PCA3 lncRNA in the tumoral cell line LNCaP. Moreover, unlike the commercial FDA-approved test, this methodology enables the detection of PCA3 lncRNA in urine samples from patients diagnosed with PCa without a previous RNA amplification. For these clinical samples we found a current intensity ratio similar to that recorded in androgen-sensitive tumoral cell lines. Analysis of a larger number of samples is needed to establish a ratio cut-off with clinical utility in the diagnosis and/or stratification of PCa patients.

CRedit authorship contribution statement

Raquel Sánchez-Salcedo: Methodology, Investigation, Data curation, Writing – original draft, Writing – review & editing. **Rebeca Miranda-Castro:** Supervision, Conceptualization, Data curation, Methodology, Writing – original draft, Writing – review & editing. **Noemí de-los-Santos-Álvarez:** Conceptualization, Supervision, Data curation, Methodology, Writing – review & editing. **María Jesús Lobo-Castañón:** Conceptualization, Resources, Project administration, Supervision, Writing – review & editing.

Declaration of competing interest

The authors declare that they have no known competing financial interests or personal relationships that could have appeared to influence the work reported in this paper.

Acknowledgments

The authors wish to thank Dr. Jesus M. Fernández Gómez and Jorge García Rodríguez from the Department of Urology (Hospital Universitario Central de Asturias, HUCA) for providing the urine samples,

and to Dr. M. Belen Prieto García and Daniel Al Kassam from the Medicine Laboratory (HUCA) for performing the initial urine sample pretreatment. We also thank Dr. Rosa M. Sainz (Departamento de Morfología y Biología Celular, Universidad de Oviedo) for her kind donation of PC-3 cells and DHT, and Dr. M. García-Ocaña (Servicios Científico-Técnicos, Universidad de Oviedo) for his technical assistance with cell cultures and electrophoretic analysis of RNA.

The work was funded by the Spanish Government (RTI-2018-095756-B-I00), and Principado de Asturias Government (IDI2018-000217), co-financed by FEDER funds. R.S.S. thanks the Spanish Ministerio de Ciencia, Innovación y Universidades for a predoctoral grant FPI (MCIU-20-PRE2019-087618).

Appendix A. Supplementary data

Supplementary data to this article can be found online at <https://doi.org/10.1016/j.bios.2021.113520>.

References

- Barreda-García, S., Miranda-Castro, R., de-los-Santos-Álvarez, N., Lobo-Castañón, M.J., 2018. *Sensor. Actuator. B Chem.* 268, 438–445.
- Bellassai, N., Spoto, G., 2016. *Anal. Bioanal. Chem.* 408, 7255–7264.
- Bhan, A., Soleimani, M., Mandal, S.S., 2017. *Canc. Res.* 77, 3965–3981.
- Bussemakers, M.J., van Bokhoven, A., Verhaegh, G.W., Smit, F.P., Karthaus, H.F., Schalken, J.A., Debruyne, F.M., Ru, N., Isaacs, W.B., 1999. *Canc. Res.* 59, 5975–5979.
- Catalona, W.J., 2018. *Med. Clin. North. Am.* 102, 199–214.
- Das, J., Kelley, S.O., 2020. *Angew. Chem., Int. Ed. Engl.* 59, 2554–2564.
- de Kok, J.B., Verhaegh, G.W., Roelofs, R.W., Hessels, D., Kiemeny, L.A., Aalders, T.W., Swinkels, D.W., Schalken, J.A., 2002. *Canc. Res.* 62, 2695–2698.
- Ferreira, L.B., Palumbo, A., Duarte de Mello, K., Sternberg, C., Caetano, M.S., Leite de Oliveira, F., Freitas-Neves, A., Nasciutti, L.E., Goulart, L.R., Rodrigues-Pereira-Gimba, E., 2012. *BMC Canc.* 12, 507.
- Fu, X., Wen, J., Li, J., Lin, H., Liu, Y., Zhuang, X., Tian, C., Chen, L., 2019. *Nanoscale* 11, 15550–15536.
- Groskopf, J., Aubin, S.M.J., Deras, I.L., Blase, A., Bodrug, S., Clark, C., Brentano, S., Mathis, J., Pham, J., Meyer, T., Cass, M., Hodge, P., Macairan, M.L., Marks, L.S., Rittenhouse, H., 2006. *Clin. Chem.* 52, 1089–1095.
- Hessels, D., Gunnewiek, J.M.T.K., van Oort, I., Karthaus, H.F.M., van Leenders, G.J.L., van Balken, B., Kiemeny, L.A., Witjes, J.A., Schalken, J.A., 2003. *Eur. Urol.* 44, 8–16.
- Htoo, K.P.P., Yamkamon, V., Yainoy, S., Suksrichavalit, T., Viseshsindh, W., Eiamphungporn, W., 2019. *Clin. Chim. Acta* 488, 40–49.
- Labib, M., Sargent, E.H., Kelley, S.O., 2016. *Chem. Rev.* 116, 9001–9090.
- Lemos, A.E.G., Matos, A.D.R., Ferreira, L.B., Gimba, E.R.P., 2019. *Oncotarget* 10, 6589–6603.
- Livak, K.J., Schmittgen, T.D., 2001. *Methods* 25, 402–408.
- Magklara, A., Scorilas, A., Stephan, C., Kristiansen, G.O., Hauptmann, S., Jung, K., Diamandis, E.P., 2000. *Urology* 56, 527–532.
- Meng, F.J., Shan, A., Jin, L., Young, C.Y.F., 2002. *Canc. Epidemiol. Biomarkers Prev.* 11, 305–309.
- Miranda-Castro, R., de-los-Santos-Álvarez, P., Lobo-Castañón, M.J., Miranda-Ordieres, A. J., Tuñón-Blanco, P., 2007. *Anal. Chem.* 79, 4050–4055.
- Miranda-Castro, R., de-los-Santos-Álvarez, N., Lobo-Castañón, M.J., 2018. *Electroanalysis* 30, 1229–1240.
- Miranda-Castro, R., de-los-Santos-Álvarez, N., Lobo-Castañón, M.J., 2019. *Anal. Bioanal. Chem.* 411, 4265–4275.
- Miranda-Castro, R., Palchetti, I., de-los-Santos-Álvarez, N., 2020. *Front. Chem.* 8, 143.
- Peng, M., Chen, C., Hulbert, A., Brock, M.V., Yu, F., 2017. *Oncotarget* 8, 69162–69173.
- Rodrigues, V.C., Soares, J.C., Soares, A.C., Braz, D.C., Melendez, M.E., Ribas, L.C., Scabini, L.F.S., Bruno, O.M., Carvalho, A.L., Reis, R.M., Sanfelice, R.C., Oliveira Jr., O.N., 2021. *Talanta* 222, 121444.
- Sartori, D.A., Chan, D.W., 2014. *Curr. Opin. Oncol.* 26, 259–264.
- Siooss, J.A., Bhiladvala, R.B., Pan, W., Li, M., Patrick, S., Xin, P., Dean, S.L., Keating, C.D., Mayer, T.S., Clawson, G.A., 2012. *Nanomedicine: NBM (NMR Biomed.)* 8, 1017–1025.
- Soares, J.C., Soares, A.C., Rodrigues, V.C., Melendez, M.E., Santos, A.C., Faria, E.F., Reis, R.M., Carvalho, A.L., Oliveira, O.N., 2019. *ACS Appl. Mater. Interfaces* 11, 46645–46650.
- Sung, H., Ferlay, J., Siegel, R.L., Laversanne, M., Soerjomataram, I., Jemal, A., Bray, F., 2021. *CA cancer. J. Clin.* 71, 209–249.
- Tai, S., Sun, Y., Squires, J.M., Zhang, H., Oh, W.K., Liang, C.-Z., Huang, J., 2011. *Prostate* 71, 1668–1679.
- Vargas, E., Povedano, E., Krishnan, S., Teymourian, H., Tehrani, F., Campuzano, S., Dassau, E., Wang, J., 2020. *Biosens. Bioelectron.* 167, 112512.
- Vilela, P., El-Sagheer, A., Millar, T.M., Brown, T., Muskens, O.L., Kanaras, A.G., 2017. *ACS Sens.* 2, 52–56.
- Wang, L.X., Fu, J.J., Zhou, Y., Chen, G., Fang, C., Lu, Z.S., Yu, L., 2020. *Talanta* 208, 120407.
- Zuker, M., 2003. *Nucleic Acids Res.* 31, 3406–3415.